INTERNATIONAL JOURNAL OF ADAPTIVE CONTROL AND SIGNAL PROCESSING
Int. J. Adapt. Control Signal Process. 2016; **30**:429–442
Published online 1 July 2015 in Wiley Online Library (wileyonlinelibrary.com). DOI: 10.1002/acs.2583

Multi-component instantaneous frequency estimation using locally adaptive directional time frequency distributions

Nabeel Ali Khan*,† and Boualem Boashash‡

Department of Electrical Engineering, Qatar University, Doha, Qatar

SUMMARY

This paper presents a locally adaptive time-frequency (t, f) method for estimating the instantaneous frequency (IF) of multi-component signals. A high-resolution adaptive directional time-frequency distribution (ADTFD) is defined by locally adapting the direction of its smoothing kernel at each (t, f) point based on the direction of the energy distribution in the (t, f) domain. The IF of signal components is then estimated from the ADTFD using an image processing algorithm. Using the mean square error between the original IF and estimated IF as a performance criterion, experimental results indicate that the ADTFD gives better IF estimation performance compared with other TFDs for a multi-component signal. For example, for signal-to-noise ratio of 12 dB, the IF estimate obtained using the ADTFD achieves a mean square error of −42 dB for a weak signal component, which is an improvement of −12 dB compared with other TFDs. Copyright © 2015 John Wiley & Sons, Ltd.

Received 29 October 2014; Revised 30 April 2015; Accepted 23 May 2015

KEY WORDS: adaptive time-frequency distribution; multi-component signals; instantaneous frequency estimation; directional kernel; local adaptation

1. INTRODUCTION

The instantaneous frequency (IF) is a key parameter for the analysis of non-stationary real-life signals such as sonar, radar, biomedical, telecommunication, fault detection and others [1–4]. Many non-stationary signals can be modelled using the amplitude modulated frequency modulated representation given in the following [5].

$$s(t) = \sum_{k=1}^{M} s_k(t) = \sum_{k=1}^{M} a_k(t) cos(\phi_k(t)) \tag{1}$$

where $s(t)$ is a multi-component signal, M is the number of signal components, $a_k(t)$ is the amplitude of the kth signal component and $\phi_k(t)$ is the instantaneous phase of the signal. It is assumed that $a_k(t)$ is a low-frequency signal whose spectrum does not overlap with the high-frequency component $cos(\phi_k(t))$ [6]. The IF of a signal component is defined as the time derivative of the instantaneous phase of the signal component [7].

$$f_k(t) = \frac{d}{dt}\phi_k(t) \tag{2}$$

Non-stationary signals can be classified into mono-component signals (i.e. $M = 1$) and multi-component signals (i.e. $M > 1$). A mono-component signal appears as a single ridge in the (t, f) domain whereas a multi-component signal appears as multiple ridges in the time-frequency (t, f)

*Correspondence to: Nabeel Ali Khan, Department of Electrical Engineering, Qatar University, Doha, Qatar.
†E-mail: nabeelalikhan@qu.edu.qa; nabeel.alikhan@gmail.com
‡The University of Queensland, UQ Centre for Clinical Research, Brisbane, Australia. E-mail: boualem@qu.edu.qa

domain [8]. Time-frequency distributions (TFDs) are often used to estimate the IF of non-stationary signals because of their robustness to distributed noise. The IF of a mono-component signal can be estimated by detecting the location of peaks along the frequency axis in a TFD [8]. The Wigner Ville distribution (WVD) gives an ideal estimate for mono-component linearly frequency modulated (LFM) signals, but its estimate is biased for non-linear FM signals [8, 9]. Adaptive algorithms based on the intersection of confidence interval (ICI) rule have shown to improve the accuracy of the WVD for non-linear FM signals at high signal-to-noise ratio (SNR) [10]. In order to estimate the IF at low SNR, the Viterbi algorithm or method based on the adaptive combination of directionally smoothed WVDs can be employed [11, 12].

The IF of a multi-component signal can also be estimated by first extracting the signal components from the (t, f) domain using a blind source separation algorithm and then estimating the IFs of extracted components using the ICI or modified ICI rule [13, 14]. The component extraction procedure requires prior information regarding the total number of components or SNR. Another approach is to use an image processing algorithm based on linking connected components to estimate the IF of multi-component signals from the (t, f) domain [15]. Only those components appearing for a duration longer than a predetermined threshold are retained. So, the algorithm does not require prior information regarding the total number of signal components or SNR. This algorithm was used for the analysis of biomedical signals such as heart rate variability and newborn electroencephalograph (EEG) signals [2, 16].

The aforementioned and other previous studies have shown that the performance of multi-component IF estimation algorithms depend on the ability of a TFD to resolve closely spaced signal components [17]. This requirement can be met by designing high-resolution TFDs. An approach is to use separable kernel TFDs such as the Extended Modified B distribution (EMBD), as they are easier to implement and offer higher resolution as compared with that of the Spectrogram because of their flexibility to independently control smoothing along the frequency axis and time axis [18, 19]. However, such separable kernel TFDs fail to concentrate energy for signals whose energy is distributed along a certain direction in the (t, f) plane, as these methods do not have any parameter to adapt the direction of their smoothing kernels [18]. For such signals, directional filtering can lead to a better compromise between cross-term suppression and auto-term resolution [18, 20, 21]. Existing directional filtering techniques use a single directional kernel for all the points in a TFD and do not make any local adaptations [21]. So these methods are not applicable for signals with multiple directions of energy distribution in the (t, f) domain such as EEG seizure signals. In order to overcome the problems associated with designing a single global kernel for all points in the (t, f) plane, adaptive kernel TFDs have been developed including the adaptive optimal kernel TFD (AOK-TFD) and adaptive fractional spectrogram (AFS) [17, 22]. Both of these latter methods are limited, as they fail to concentrate energy when there is a significant variation in the amplitudes of signal components.

This paper defines a novel locally adaptive directional TFD (ADTFD) that can resolve closely spaced signal components without degrading the resolution of weak signal components. Experimental results indicate that the ADTFD outperforms other adaptive and fixed kernel TFDs in terms of its ability to accurately estimate the IF of a multi-component signal with varying amplitudes and chirp rates. The paper is organized as follows. Section 2 defines the ADTFD. Section 3 describes the IF estimation algorithm. Experimental results are discussed in Section 4. Finally, Section 5 concludes the paper.

2. THE ADAPTIVE DIRECTIONAL KERNEL

2.1. Definition and analysis of the adaptive directional time-frequency distribution

Previous studies have shown that filtering along the direction of the energy concentration of linearly frequency modulated signal components can be used to obtain a high-resolution TFD with a significant suppression of cross-terms [21]. A limitation of these methods is that they cannot give optimal performance for signals with non-linear IF variations as such signals do not have one specific direction of energy distribution in the (t, f) domain. So, one way to remedy the limitation is to ensure that the direction of the kernel is adapted locally at each (t, f) point. In this study, we define a new

DOI: 10.1002/acs

ADTFD that uses the direction of local energy distribution of a signal in the (t, f) domain to adapt its smoothing kernel.

The ADTFD is defined as the 2D convolution of a quadratic TFD with an adaptive directional filter.

$$\rho_{(adapt)}(t, f) = \rho(t, f) \underset{t}{*} \underset{f}{*} \gamma_\theta(t, f) \tag{3}$$

where $\gamma_\theta(t, f)$ is the adaptive directional kernel, whose shape depends on the parameter θ that is adapted at each point in a (t, f) plane, $\rho(t, f)$ is a quadratic TFD defined as the 2D convolution of the WVD with a 2D smoothing kernel:

$$\rho(t, f) = W_z(t, f) \underset{t}{*} \underset{f}{*} \gamma(t, f) \tag{4}$$

$W_z(t, f)$ is the WVD of $z(t)$, which is the analytic associate of a real signal $s(t)$. The WVD is defined as:

$$W_z(t, f) = \int z\left(t + \frac{\tau}{2}\right) z^*\left(t - \frac{\tau}{2}\right) e^{-j2\pi f\tau} d\tau \tag{5}$$

The criterion to adapt the shape of the directional kernel is based on the following characteristics of cross-terms and auto-terms in quadratic TFDs [23]:

1. Cross-terms oscillate along their major axis. This implies that cross-terms can be suppressed by smoothing them along their major axis as cross-terms have high pass characteristics in the frequency domain.
2. The amplitude of auto-terms changes slowly along their major axis. This implies that low pass filtering along the major axis of auto-terms will not deteriorate their energy concentration. The reason is that most of the auto-term energy lies in a low frequency band because of the slow variation in the amplitude of auto-terms.

In order to suppress cross-terms without affecting the resolution of auto-terms, the direction of a smoothing kernel should remain aligned with the major axis of auto-terms and cross-terms. For auto-term points, the direction of a smoothing kernel can be estimated by choosing an angle that maximizes the correlation of a directional filter with a quadratic TFD. This approach cannot be used for cross-term points, given that the correlation of a directional filter with cross-terms would result in zero because of the oscillatory characteristics of cross-terms. The oscillatory characteristics of cross-terms can be avoided by taking the modulus of a quadratic TFD. For absolute values of a TFD, both auto-terms and cross-terms appear as ridges. So, the direction of a smoothing kernel for any given (t, f) point can be estimated by maximizing the correlation of the directional kernel with the modulus of a quadratic TFD.

$$\theta(t, f) = \arg\max_{\theta} \left| |\rho(t, f)| \underset{t}{*} \underset{f}{*} \gamma_\theta(t, f) \right| \tag{6}$$

In the aforementioned expression, the oscillatory effect of cross-terms is removed from the $\rho(t, f)$ TFD by taking its modulus. The directional filter $\gamma_\theta(t, f)$ is not squared to avoid change in shape of the chosen directional filter. Note that the modulus of a TFD is only used for estimating the local direction of the smoothing kernel $\theta(t, f)$. Once $\theta(t, f)$ is estimated, the smoothing is performed in the normal (t, f) domain as expressed in Eq. 3.

2.2. *Constraints on the smoothing kernel* $\gamma_\theta(t, f)$

The earlier discussion indicates that the smoothing kernel should have the following properties.

(i) It should have maximum output when it is parallel to ridges so that direction of these ridges is correctly estimated using Eq. 6. This implies the kernel should be a low pass filter along its major direction.
(ii) The output of the smoothing kernel should be zero when it is not parallel to ridges, so that we do not observe energy at those points where no signal component is present.

DOI: 10.1002/acs

It is known that even derivatives of the directional Gaussian filters approximately fulfill the aforementioned properties [24]. Their output is maximum when their direction is along the ridges, while their response reduces to zero as their direction is rotated along the direction orthogonal to ridges [24, 25]. In this study, we have selected the double derivative directional Gaussian filter (DGF) as it meets the aforementioned criteria with simplicity and ease of implementation [24].

$$\gamma_\theta(t, f) = \frac{ab}{2\pi}\frac{d^2}{df_\theta^2}e^{-a^2t_\theta^2-b^2f_\theta^2} \tag{7}$$

where $t_\theta = t\cos(\theta) + f\sin(\theta)$, $f_\theta = -t\sin(\theta) + f\cos(\theta)$, θ is the rotation angle with respect to the time-axis and a and b control the spread of the DGF along the time or frequency axis, respectively. The parameter a controls smoothing along the major axis, while the parameter b controls smoothing along the minor axis. Eq. 7 meets the aforementioned criteria of the smoothing kernel because of the following properties.

(i) It performs smoothing along its major axis. $\left(i.e.e^{-a^2t_\theta^2}\right)$.

(ii) It performs second-order differentiation along its minor axis $\left(i.e.\frac{d^2}{df_\theta^2}e^{-b^2f_\theta^2}\right)$. So, the filter output reduces to zero as the direction of filter is made orthogonal to the major axis of ridges.

2.3. Selection of parameters for the directional Gaussian filter

The choice of parameters is based on the principle that the rate of oscillation of cross-terms decreases as signal components are brought closer in the (t, f) domain [23]. So, a long filter (with sharp cuttoff) should be applied along the major axis of ridges for suppressing cross-terms, whereas a short filter should be applied in the direction orthogonal to the major axis of ridges, so that smoothing does not merge close components. This implies that parameter a should be assigned a small value (i.e. around 2) to ensure a long filter and that parameter b should be assigned a large value (i.e. around 30) to ensure a short filter. For these reasons, the values used in this study for the parameters in Eq. 7 are $a = 2$ and $b = 30$.

2.4. Algorithm for the implementation of the adaptive directional time-frequency distribution

The key steps for the discrete time implementation of the proposed ADTFD are given in the following and illustrated in Figure 1.

- The windowed WVD is computed using the following expression:

$$W_z[n,k] = 2\sum_{m=-M/2}^{M/2} w[m]z[n+m]z^*[n-m]e^{-j2\pi mk} \tag{8}$$

  where $w[m]$ is a lag window with length $M + 1$. For the online implementation, we have used the w-WVD, instead of the WVD, as the computation of the w-WVD does not require accumulation of the complete signal.
- The w-WVD is convolved with a 2D smoothing kernel to obtain a quadratic TFD.

$$\rho[n,k] = W_z[n,k] \underset{n}{*}\underset{k}{*}\gamma[n,k] \tag{9}$$

- The modulus of a quadratic TFD is convolved with a predetermined number of directional filters, resulting in the following expression:

$$\widehat{\rho_l}[n,k] = |\rho[n,k]| \underset{n}{*}\underset{k}{*}\gamma_{\theta_l}[n,k] \tag{10}$$

  where $\gamma_{\theta_l}[n,k]$ is the directional kernel rotated by $2l\pi/L$ radians along the time-axis in the (t, f) domain, L represents the total number of filters and $l = 0, 1, 2, ...L - 1$.

DOI: 10.1002/acs

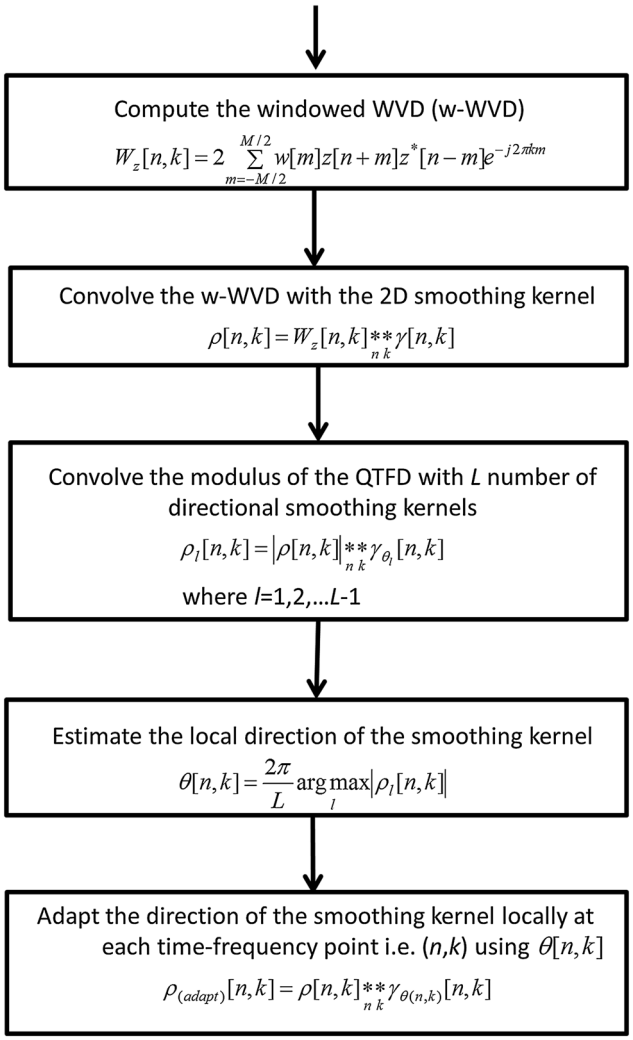

Figure 1. Algorithm for discrete time online implementation of the adaptive directional time-frequency distribution.

- For each $[n,k]$, that is, (t,f) point, the angle maximizing the correlation between the directional kernel and the modulus of TFD is selected as the optimal angle.

$$\theta[n,k]=\frac{2\pi}{L}\arg\max_l|\widehat{\rho_l}(t,f)| \tag{11}$$

  In this study, we have used 18 quantization levels, that is, $L=18$.
- The ADTFD is obtained by convolving $\rho[n,k]$ with $\gamma_\theta[n,k]$, such that the shape of $\gamma_\theta[n,k]$ is adapted locally using the $\theta[n,k]$.

$$\rho_{adapt}[n,k]=\rho[n,k]\underset{n}{*}\underset{k}{*}\gamma_\theta[n,k] \tag{12}$$

Note that the proposed algorithm can be implemented online as it does not require accumulation of the complete signal.

2.5. *Illustration of the adaptive directional time-frequency distribution*

The proposed directional adaptive kernel can be applied to any quadratic TFD, the aim being to improve the TFD energy concentration by suppressing undesired cross-terms. In order to obtain the best possible resolution, the adaptive directional kernel could directly process the WVD as all

DOI: 10.1002/acs

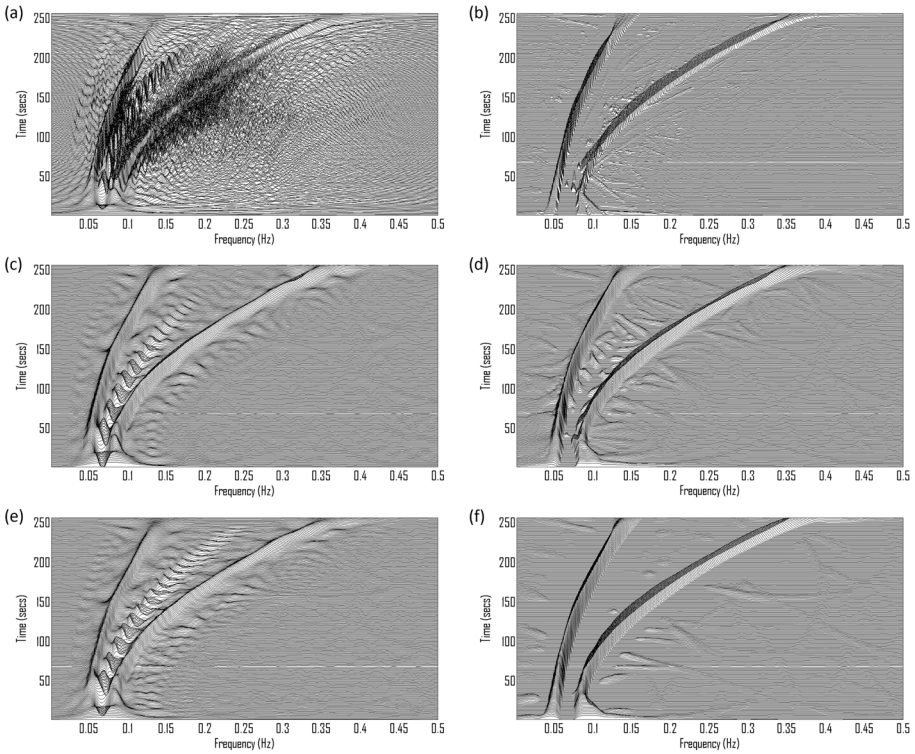

Figure 2. Illustration of the adaptive directional time-frequency distribution (ADTFD) using a two component signal: (a) the Wigner Ville distribution ; (b) The ADTFD, obtained using the WVD as underlying TFD ; (c) The S-method; (d) the ADTFD, obtained using the S-method as underlying TFD; (e) the Extended Modified B-Distribution (EMBD) ($\alpha = 0.25, \beta = 0.25$); and (f) The ADTFD, obtained using the EMBD as underlying TFD ($a = 2, b = 20$).

other TFDs distort the energy concentration of auto-terms because of 2D smoothing. However, the WVD gives poor energy concentration for noisy signals and signals with non-linear IF [26]. For such signals, the smoothed versions of the WVD give significantly better (t, f) representation, which can then be further enhanced by the proposed directional filtering. The smoothing parameters for the underlying TFD are selected to suppress noise. The smoothing should not be extensive to merge close signal components, otherwise, the proposed cross-term suppression method would fail to improve the resolution of signal components [27]. Any quadratic TFD, including the S-method, with parameters to control the extent of 2D smoothing can be selected as an underlying TFD.

Let us consider a multi-component signal composed of two quadratic FM signal components. The signal is defined as:

$$\begin{aligned} s(t) &= s_1(t) + s_2(t) && 0 \leqslant t \leqslant 255 \\ s(t) &= 0 && \textit{Otherwise} \end{aligned} \tag{13}$$

where

$$\begin{aligned} s_1(t) &= 2\cos\left(0.1\pi t + 0.000001\pi t^3\right) \\ s_2(t) &= 2\cos\left(0.15\pi t + 0.000003\pi t^3\right) \end{aligned} \tag{14}$$

The IFs of the aforementioned signal components are given in the following.

$$\begin{aligned} f_1(t) &= 0.05 + 0.0000015t^2 \\ f_2(t) &= 0.075 + 0.0000045t^2 \end{aligned} \tag{15}$$

The signal is corrupted by additive white Gaussian noise of SNR 10 dB, which is a realistic situation in many applications including EEG signal analysis [1]. Three quadratic TFDs are selected

DOI: 10.1002/acs

for validation and comparison: the WVD, the EMBD and the S-method. Cross-terms from all these TFDs are suppressed using the adaptive directional kernel as shown in Figure 2. All the ADTFDs have resolved close signal components with significant suppression of cross-terms. The ADTFD, obtained using the EMBD as the underlying method, shows the best performance in terms of suppressing cross-terms while retaining resolution and energy concentration of auto-terms.

3. MULTI-COMPONENT INSTANTANEOUS FREQUENCY ESTIMATION USING CONNECTED COMPONENT LINKING ALGORITHM

In this study, an image processing technique based on linking connected components is used to estimate the IF of a multi-component signal. This technique is selected because of its computational efficiency and good performance for real-life signals such as EEG seizure signals and heart rate variability signals as shown in [2, 16]. The key steps of the IF estimation procedure are as follows.

(i) Let us define $B(t, f)$ as a binary (t, f) image having ones on all peak locations and zeros on all other points.

(ii) Detect peaks along the frequency axis at each time instant in the (t, f) domain using the first and second-order derivatives as expressed in the following [15].

$$\begin{aligned} &B(t,f) = 1 \quad if \quad \frac{d}{df}\rho(t,f) = 0 \quad and \quad \frac{d^2}{df^2}\rho(t,f) < 0 \\ &B(t,f) = 0 \quad Otherwise \end{aligned} \tag{16}$$

(iii) The detected peaks are assumed to correspond to the IFs of signal components. The IF of signal components is extracted by using the 10-connectivity criterion described in [15]. According to this criterion, a detected peak belongs to a signal component if it has at least one other peak in its 10-neighborhood of the same signal component and it does not have a peak of any other component in its 10-neighborhood. For a detected peak at location (x, y), its 10-neighborhood is defined as the following set of points.
$(x-1, y), (x-1, y-1), (x-1, y+1), (x-1, y+2), (x-1, y-2), (x+1, y), (x+1, y-1), (x+1, y+1), (x+1, y+2), (x+1, y-2)$.
Note that the standard 8-connected neighborhood cannot be used for estimating the IF as it includes points above and below the IF curves, whereas for any given signal component, there can be only one frequency at any time instant [15]. In practical implementations, IF curves with a duration longer than a predetermined threshold are retained to improve the robustness of the algorithm against noise, as this step removes false peaks.

4. RESULTS AND DISCUSSION

4.1. Performance evaluation on synthetic signals

Let us consider a multi-component signal composed of four quadratic chirps for evaluation of the IF estimation capability of the ADTFD. There is variation in relative amplitudes of signal components, such that two components are strong while the other two components are weak. The signal can be expressed as:

$$\begin{aligned} &s(t) = s_1(t) + s_2(t) + 0.5s_3(t) + 0.5s_4(t) && 0 \leqslant t \leqslant 255 \\ &s(t) = 0 && Otherwise \end{aligned} \tag{17}$$

where

$$\begin{aligned} s_1(t) &= \cos\left(0.1\pi t + 0.000002\pi t^3\right) \\ s_2(t) &= \cos\left(0.15\pi t + 0.000002\pi t^3\right) \\ s_3(t) &= \cos\left(0.9\pi t - 0.000001\pi t^3\right) \\ s_4(t) &= \cos\left(0.95\pi t - 0.000001\pi t^3\right) \end{aligned} \tag{18}$$

DOI: 10.1002/acs

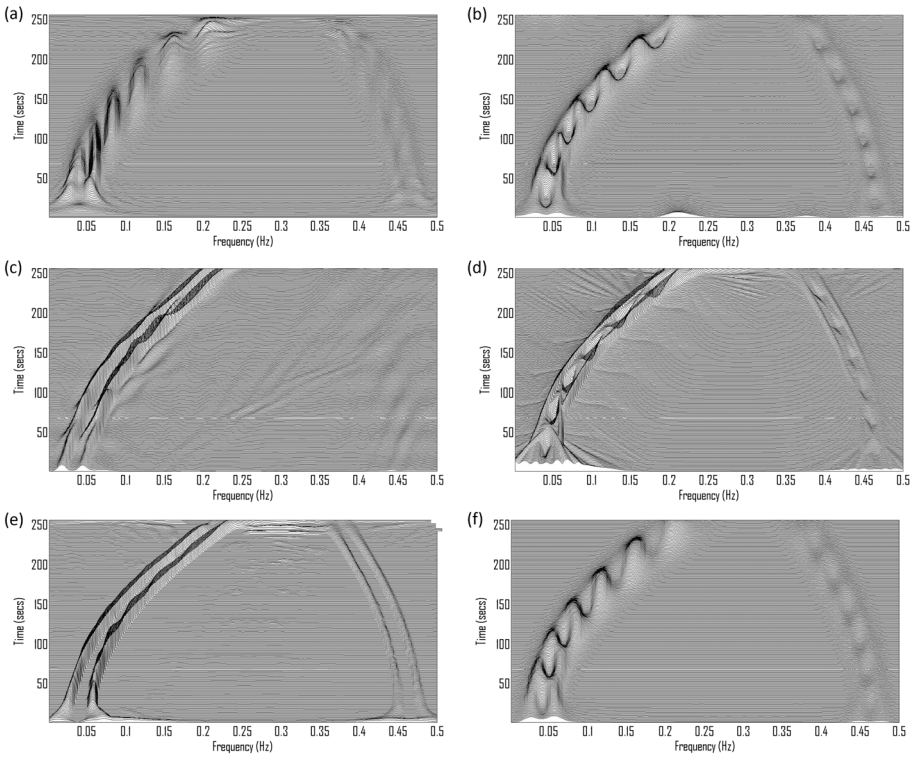

Figure 3. (a) The spectrogram ; (b) the Extended Modified B-Distribution ; (c) the adaptive optimal kernel time-frequency distribution; (d) the adaptive fractional spectrogram; (e) the adaptive directional time-frequency distribution ; and (f) the S-method (Hamming window of length 4 s).

The IFs of the aforementioned signal components are given in the following.

$$\begin{aligned} f_1(t) &= 0.05 + 0.000003t^2 \\ f_2(t) &= 0.075 + 0.000003t^2 \\ f_3(t) &= 0.45 - 0.0000015t^2 \\ f_4(t) &= 0.475 - 0.0000015t^2 \end{aligned} \tag{19}$$

This multi-component signal is sampled at 1 Hz. The signal is analysed using the spectrogram, AFS, EMBD, AOK-TFD [22], ADTFD and the S-method [28], as shown in Figure 3. For the adaptive method, we have used the EMBD as the underlying distribution, as the previous section showed that the best results are obtained using the EMBD. The parameters of the TFDs have been optimized based on visual inspection to maximize their energy concentration and resolution properties. Figure 4 shows slices extracted from the aforementioned TFDs for time instant 128.

Figures 3 and 4 show that the fixed kernel TFDs (which are the spectrogram, S-method and EMBD) have failed to resolve close signal components. The AFS has resolved the quadratic chirps, but it suffers from energy leakage between the peaks of close components. The AOK-TFD resolves the strong components, but it fails to concentrate energy for the weak signal components. The ADTFD has resolved both the strong and weak signal components without suffering from the problem of energy leakage or cross-terms.

White Gaussian noise is added to the signal. The IF of the signal is estimated using the connected component linking algorithm, described in Section 3, for SNR ranging from -5 to 12 dB. The accuracy of the IF estimates is defined as the mean square error (MSE) between the estimated IF and the original IF. The MSE is estimated by performing 100 Monte Carlo simulations [29]. The following observations can be made regarding the results of the IF estimates that are shown in Figure 5:

DOI: 10.1002/acs

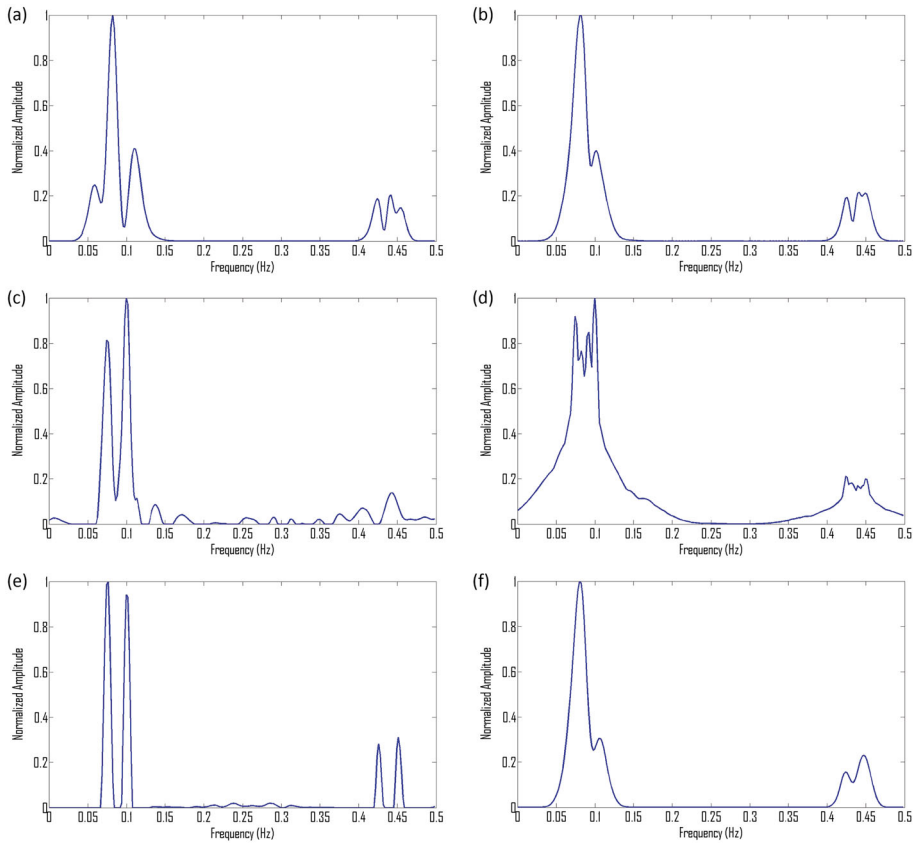

Figure 4. (a) Time slice taken from the spectrogram; (b) time slice taken from the Extended Modified B-Distribution; (c) time slice taken from the adaptive optimal kernel time-frequency distribution; (d) time slice taken from the adaptive fractional spectrogram; (e) time slice taken from the adaptive directional time-frequency distribution; and (f) time slice taken from the S-method.

(i) All fixed kernel TFDs fail to give accurate IF estimates, that is, MSE below -35 dB even at high SNR. This poor performance of fixed kernel methods is because of their inability to resolve close signal components.
(ii) The AOK-TFD gives the best performance for the strong signal components, but its performance is worst for the weak components as the AOK-TFD fails to concentrate energy for the weak components as shown in Figure 4(c).
(iii) The ADTFD is the only distribution that can be used to accurately estimate the IFs of both strong and weak signal components. For SNR greater than 2.5 dB, the ADTFD is the second best TFD for estimating the IF of strong signal components that are $s_1(t)$ and $s_2(t)$. For SNR greater than 6 dB, the ADTFD is the best TFD for estimating the IF of weak signal components that are $s_3(t)$ and $s_4(t)$. The better performance of the ADTFD is because of its high resolution and energy concentration for both strong and weak signal components as shown in Figure 4(e).

4.2. Illustration on a real life electroencephalograph seizure signal

A newborn EEG seizure signal of duration 8 s acquired at sampling frequency of 32 Hz is analysed using the ADTFD, AOK-TFD and S-method. For the ADTFD, we have used the EMBD as the underlying TFD. The IFs of its components are estimated from these distributions using the connected component linking algorithm. Figure 6 shows the TFDs and estimated IFs of the EEG seizure signal. The AOK-TFD gives high energy concentration for the stronger components, but fails to concentrate energy for the weaker components, thus resulting in a smeared (t, f) representation. The S-method gives high energy concentration for both strong and weak

DOI: 10.1002/acs

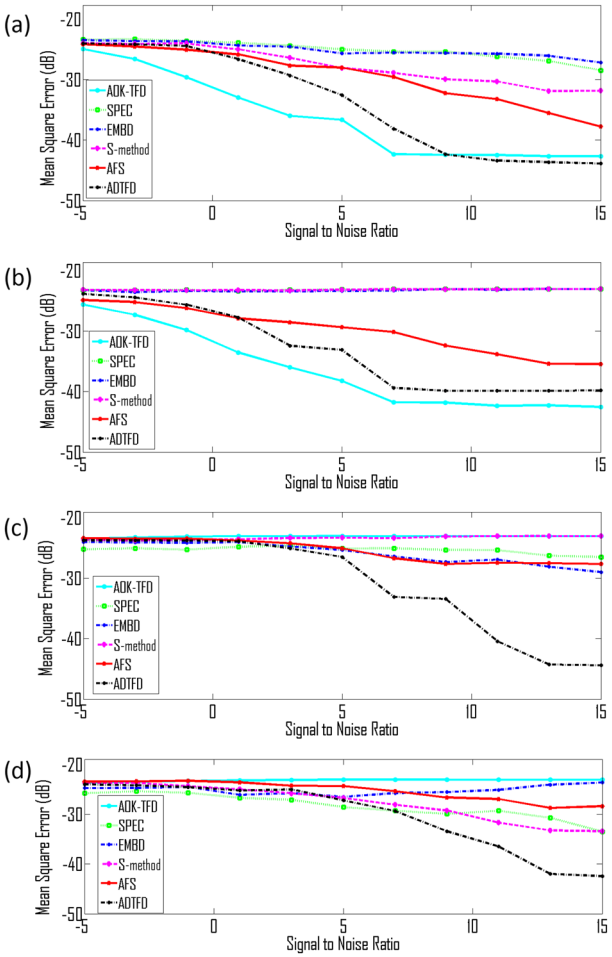

Figure 5. Mean square error (MSE) of the instantaneous frequency (IF) estimates for the multi-component signal. (a) MSE of the IF estimate of $s_1(t)$ versus signal-to-noise ratio ; (b) MSE of the IF estimate of $s_2(t)$ versus SNR; (c) MSE of the IF estimate of $s_3(t)$ versus SNR; and (d) MSE of the IF estimate of $s_4(t)$ versus SNR.

signal components, resulting in accurate IF estimates for both strong and weak signal components. Although the S-method leads to accurate IF estimates, it fails to suppress cross-terms between two close signal components. The ADTFD gives high energy concentration for both weak and strong signal components. Moreover, it does not suffer from cross-term interference problem, thus resulting in an accurate estimation of IF curves. This example illustrates that the ADTFD can be used for the analysis and IF estimation of real-life signals such as EEG seizure signals.

4.3. Discussion and interpretation of results

4.3.1. Interpretation of results. The IF estimation capability of a (t, f) method depends on the resolution and cross-term suppression properties of the TFD employed. A high-resolution TFD is required to ensure that peaks of closely spaced components are well separated, while the suppression of cross-terms is needed to remove false peaks from the (t, f) plane. The ability of the ADTFD to suppress cross-terms while resolving close components of varying amplitudes results in the accurate estimation of the IFs of both strong and weak signal components. For example, for an SNR of 12 dB, the ADTFD achieves the MSE of -42 dB for the third component, while all the other selected TFDs fail to achieve the MSE of less than -30 dB.

DOI: 10.1002/acs

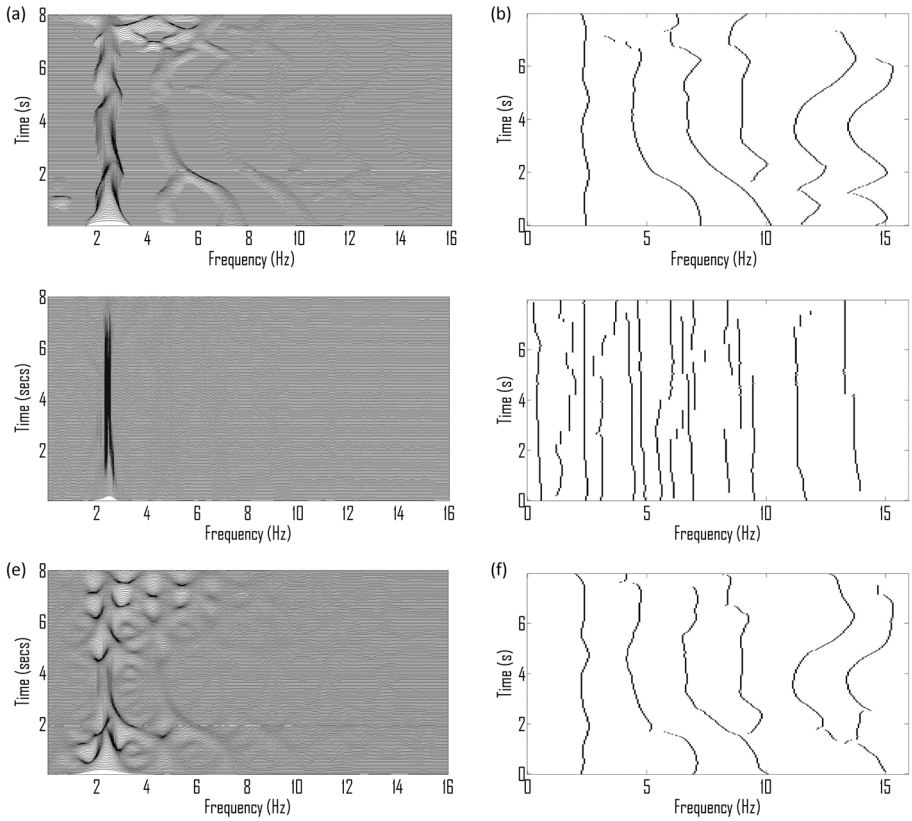

Figure 6. Illustration of the instantaneous frequency (IF) estimation technique on a newborn electroencephalograph seizure signal. (a) The adaptive directional time-frequency distribution (ADTFD); (b) the estimated IFs using the ADTFD; (c) the adaptive optimal kernel time -frequency distribution (AOK-TFD); (d) the estimated IFs using the AOK-TFD; (e) the S-method; and (f) the estimated IFs using the S-method.

4.3.2. Tradeoffs involved in the selection of parameters for the directional Gaussian filter. The performance of the ADTFD depends on the lengths of smoothing filters applied along major and minor axes of ridges. In order to resolve close signal components, the parameters must be selected to ensure that a long duration smoothing filter is applied along the major axis of ridges and that a short duration filter is applied along the minor axes, as discussed in Section 2, but such filters would spread energy for short duration signal components.

Let us consider a multi-component signal composed of two Gaussian atoms and two linearly frequency modulated signals.

$$\begin{aligned} s(t) &= s_1(t) + s_2(t) + s_3(t) + s_4(t) \qquad 0 \leqslant t \leqslant 255 \\ s(t) &= 0 \qquad\qquad\qquad\qquad\qquad\qquad\quad \textit{Otherwise} \end{aligned} \tag{20}$$

where

$$\begin{aligned} s_1(t) &= 2\cos\left(0.1\pi t + 0.0008\pi t^2\right) \\ s_2(t) &= 2\cos\left(0.04\pi t + 0.0008\pi t^2\right) \\ s_3(t) &= 2e^{-0.0015(t-64)^2}\cos\left(0.8\pi t\right) \\ s_4(t) &= 2e^{-0.0015(t-192)^2}\cos\left(0.8\pi t\right) \end{aligned} \tag{21}$$

The IFs of the aforementioned signal components are given in the following.

$$\begin{aligned} f_1(t) &= 0.05 + 0.0004t \\ f_2(t) &= 0.02 + 0.0004t \\ f_3(t) &= 0.4 \\ f_4(t) &= 0.4 \end{aligned} \tag{22}$$

DOI: 10.1002/acs

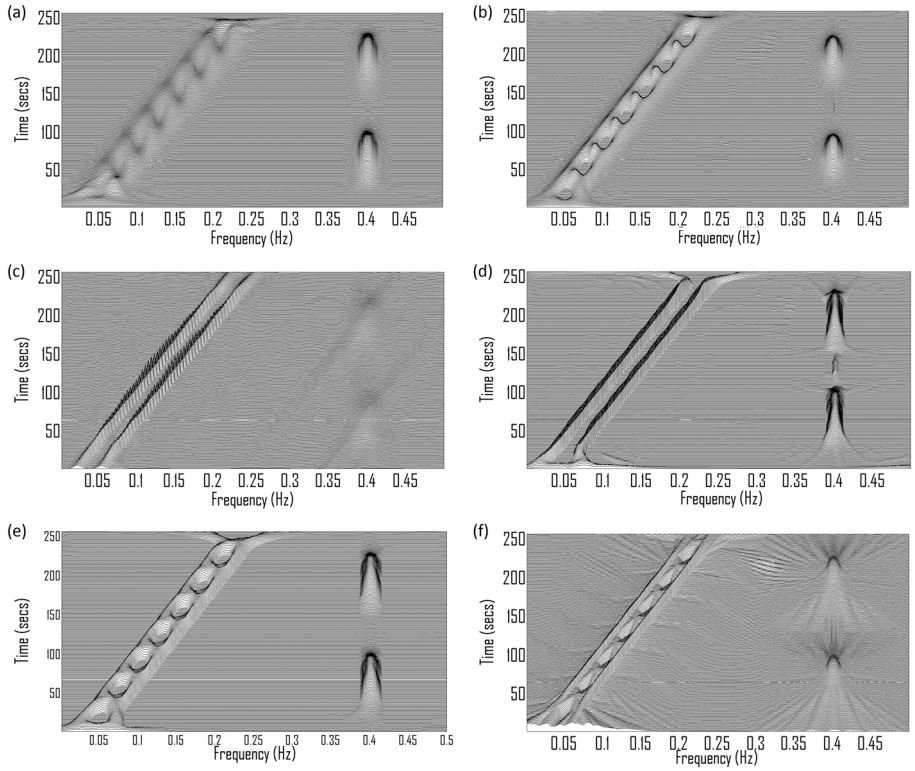

Figure 7. (a) The spectrogram (Hamming window length 85 s); (b) the Extended Modified B-Distribution ($\alpha = 0.1, \beta = 0.1$); (c) the adaptive optimal kernel time-frequency distribution; (d) the adaptive directional time-frequency distribution (ADTFD) ($a = 2, b = 20$); (e) the ADTFD ($a = 3, b = 8$); and (f) the adaptive fractional spectrogram .

This signal is analyzed using the spectrogram, EMBD, ADTFD, AOK-TFD and AFS as shown in Figure 7. The EMBD and spectrogram have failed to resolve the two close LFM components. The AOK-TFD has resolved the LFM components, but it spreads signal energy for the two Gaussian atoms. The AFS suffers from energy leakage between signal components. In case of the ADTFD, there is a tradeoff to either resolve the LFM components or maintain the time-support of Gaussian atoms. The ADTFD with parameters ($a = 2, b = 20$) resolves the close components, but it spreads signal energy for the two Gaussian atoms, that is, we can see energy between the two Gaussian atoms in Figure 7(d). The ADTFD with parameters ($a = 3, b = 8$) maintains the energy concentration of the Gaussian atoms but fails to resolve the LFM components. This limitation of the ADTFD can be overcome by locally adapting the size of the DGF. For example, the length of the DGF should increase in the region occupied by the LFM signals, while its length should decrease in the region occupied by the Gaussian atoms.

5. CONCLUSION

This paper presented an adaptive algorithm for estimating the IF of multi-component signals of varying amplitudes. The proposed algorithm is based on a locally ADTFD that can resolve closely spaced components without degrading the energy concentration of weak components. The performance of the ADTFD is illustrated on both synthetic and real-life EEG seizure signals. The MSE between the estimated IF and original IF is used as a performance measure to compare the IF estimation capability of the ADTFD with other related methods such as the AFS. Comparative experimental results indicate that the ADTFD is the overall best performing TFD among a wide basket of TFDs, as it can be used to estimate the IF of both strong and weak signal components simultaneously, whereas the other TFDs fail to estimate the IF of weak components even at high SNR. For example, for an SNR

DOI: 10.1002/acs

of 12 dB, the ADTFD achieves an MSE of −42 dB for the third component, while all the other TFDs fail to achieve the MSE of less than −30 dB. This improved performance of the ADTFD is because of the property of local optimization of its kernel at each (t, f) point, which results in the high energy concentration observed for all the signal components including the weak ones as illustrated in Figure 3.

ACKNOWLEDGEMENTS

This work was supported by the Qatar National Research fund under its National Research Program (Award No. 4-1303-2-517 and Award No. 6-885-2-364).

REFERENCES

1. Boashash B, Azemi G, O'Toole J. Time-frequency processing of nonstationary signals: advanced TFD design to aid diagnosis with highlights from medical applications. *IEEE Signal Processing Magazine* 2013; **30**(6):108–119.
2. Dong S, Boashash B, Azemi G, Lingwood BE, Colditz PB. Automated detection of perinatal hypoxia using time-frequency-based heart rate variability features. *Medical and Biological Engineering and Computing* 2014; **52**(2): 183–191.
3. Orovic I, Stankovic S, Thayaparan T, Stankovic L. Multiwindow S-method for instantaneous frequency estimation and its application in radar signal analysis. *IET Signal Processing* 2010; **4**(4):363–370.
4. Yang S, Zhao Q. Real-time frequency estimation for sinusoidal signals with application to robust fault detection. *International Journal of Adaptive Control and Signal Processing* 2013; **27**(5):386–399.
5. Boashash B. *Advances in Spectral Analysis and Array Processing*. Prentice Hall: Cliffs, Englewood, 1991.
6. Bedrosian E. A product theorem for Hilbert transforms. *Proceedings of the IEEE* 1963; **51**(5):868–869.
7. Boashash B. Estimating and interpreting the instantaneous frequency of a signal. I. Fundamentals. *Proceedings of the IEEE* 1992; **80**(4):520–538.
8. Boashash B. *Time-Frequency Signal Analysis and Processing: A Comprehensive Reference*. Elsevier: Oxford, 2003.
9. Katkovnik V, Stankovic L. Instantaneous frequency estimation using the Wigner distribution with varying and data-driven window length. *IEEE Transactions on Signal Processing* 1998; **46**(9):2315–2325.
10. Lerga J, Sucic V. Nonlinear IF estimation based on the pseudo WVD adapted using the improved sliding pairwise ICI rule. *IEEE Signal Processing Letters* 2009; **16**(11):953–956.
11. Shui PL, Shang HY, Zhao YB. Instantaneous frequency estimation based on directionally smoothed pseudo-Wigner-Ville distribution bank. *IET Radar, Sonar and Navigation* 2007; **1**(4):317–325.
12. Djurovi I. Viterbi algorithm for chirp-rate and instantaneous frequency estimation. *Signal Processing* 2011; **91**(5):1308–1314.
13. Lerga J, Sucic V, Boashash B. An efficient algorithm for instantaneous frequency estimation of nonstationary multicomponent signals in low SNR. *EURASIP Journal on Advances in Signal Processing* 2011; **2011**(1):1–16.
14. Sucic V, Lerga J, Boashash B. Multicomponent noisy signal adaptive instantaneous frequency estimation using components time support information. *IET Signal Processing* 2014; **8**(3):277–284.
15. Rankine L, Mesbah M, Boashash B. IF estimation for multicomponent signals using image processing techniques in the time-frequency domain. *Signal Processing* 2007; **87**(6):1234–1250.
16. Boashash B, Azemi G, Khan N. Principles of time frequency feature extraction for change detection in non-stationary signals: applications to newborn EEG abnormality detection. *Pattern Recognition* 2015; **48**(3):616–627.
17. Khan N, Boashash B. Instantaneous frequency estimation of multicomponent nonstationary signals using multiview time-frequency distributions based on the adaptive fractional spectrogram. *IEEE Signal Processing Letters* 2013; **20**(2):157–160.
18. Boashash B, Khan N, Ben-Jabeur T. Time-frequency features for pattern recognition using high-resolution tfds: a tutorial review. *Digital Signal Processing* 2015; **40**:1–30.
19. Abed M, Belouchrani A, Cheriet M, Boashash B. Time-frequency distributions based on compact support kernels: properties and performance evaluation. *IEEE Transactions on Signal Processing* 2012; **60**(6):2814–2827.
20. Zheng L, Shi D, Zhang J. Caffrft: A center-affine-filter with fractional Fourier transform to reduce the cross-terms of Wigner distribution. *Signal Processing* 2014; **94**(0):330–338.
21. Bastiaans M, Alieva T, Stankovic L. On rotated time-frequency kernels. *IEEE Signal Processing Letters* 2002; **9**(11):378–381.
22. Jones D, Baraniuk R. An adaptive optimal-kernel time-frequency representation. *IEEE Transactions on Signal Processing* 1995; **43**(10):2361–2371.
23. Hlawatsch F. Interference terms in the Wigner distribution. *Digital Signal Processing* 1984; **84**:363–367.
24. Liu Y, Mejias L, Li Z. Fast power line detection and localization using steerable filter for active UAV guidance. *Proceedings of 12th International Society for Photogrammetry and Remote Sensing (ISPRS2012)*, Melbourne, Australia, 2012; 491–496.
25. Jacob M, Unser M. Design of steerable filters for feature detection using canny-like criteria. *IEEE Transactions on Pattern Analysis and Machine Intelligence* 2004; **26**(8):1007–1019.

DOI: 10.1002/acs

26. Stankovic L. Analysis of noise in time-frequency distributions. *IEEE Signal Processing Letters* 2002; **9**(9):286–289.
27. Stankovic L. Auto-term representation by the reduced interference distributions: a procedure for kernel design. *IEEE Transactions on Signal Processing* 1996; **44**(6):1557–1563.
28. Stankovic L. A method for time-frequency analysis. *IEEE Transactions on Signal Processing* 1994; **42**(1):225–229.
29. Sobol IM. *Simulation and the Monte Carlo Method*. CRC Press: Hoboken, New Jersey, 2008.

DOI: 10.1002/acs